



Cite this: *New J. Chem.*, 2021, 45, 11495

# Nucleofugality hierarchy, in the aminolysis reaction of 4-cyanophenyl 4-nitrophenyl carbonate and thionocarbonate. Experimental and theoretical study†

Rodrigo Montecinos,<sup>ib</sup>\* Margarita E. Aliaga,<sup>ib</sup> Paulina Pavez,<sup>ib</sup> Patricio Cornejo and José G. Santos<sup>ib</sup>\*

Received 30th November 2020,  
Accepted 2nd June 2021

DOI: 10.1039/d0nj05837h

rsc.li/njc

Nucleophilic substitution reactions of the title compounds have been investigated with a series of secondary alicyclic amines in several solvents. The solvent, amine, and electrophilic group effects on kinetics, mechanism and nucleofugality hierarchy are discussed from experimental and theoretical studies. These studies show the mechanistic dependence on the solvent polarity; the theoretical results indicate that the relative polarization of the reactive centres (C=O and C=S) and the stabilization of the nucleofuges are the main factors in the control of the product distribution.

## Introduction

Nucleofuge hierarchy has been established by the Mayr, Denegri and Kronja groups,<sup>1</sup> whose study involved a leaving group ability scale based on the S<sub>N</sub>1 solvolysis reactions of benzhydryl derivatives, which yield a carbocation and the nucleofuge. However, despite the large number of nucleofuge families tested,<sup>1a</sup> only a few phenols have been studied.<sup>2</sup> As the rate constants of these reactions are affected by the solvent, these nucleofugality values correspond to the nucleofuge–solvent pair.<sup>1,2</sup>

In general, we are interested in the study of nucleofugality hierarchies involved in nucleophilic reactions, *e.g.* nucleophilic substitutions through an addition–elimination mechanism, in which nucleofuge departure is not necessarily involved in the rate-determining step.

The nucleophilic substitution reactions of carbonyl and thiocarbonyl derivatives in a solution with reagents of varying nucleophilicity have been studied by several groups. In particular, kinetic and mechanism studies of these processes have been fully described,<sup>3–7</sup> but very few studies have been done on the nucleofugality hierarchy in the nucleophilic reactions of diarylcarbonates or its sulfur (thiol or thiono) and dithio analogs.

In relation to the nucleophilic reactions of diarylthiol- and diaryldithio carbonates, different nucleofuge families are involved (phenolates and benzenethiolates);<sup>7</sup> some studies show that both groups are nucleofuges. For example, in the stepwise reaction of

*O*-(4-nitrophenyl) *S*-4-(nitrophenyl) thiol (**1**) and dithiocarbonates (**2**) with secondary alicyclic amines (SAA), in aqueous ethanol, both phenoxides are nucleofuges,<sup>7b</sup> although the p*K*<sub>a</sub> of 4-nitrophenol is three units greater than the p*K*<sub>a</sub> of 4-nitrobenzenethiol.<sup>7i</sup>

In addition, the kinetic study of the reactions of **2** with a series of anilines shows that both (phenolate and benzenethiolate) are nucleofuges.<sup>7j</sup> However, in the pyridinolysis of **2**, only 4-nitrophenolate is the nucleofuge,<sup>7k</sup> suggesting that the nature of the amine affects the relative nucleofugality of groups. Also, the aminolysis of *S*-phenyl and *S*-(4-chlorophenyl) *O*-(4-nitrophenyl) thiol (**3** and **4**) and dithiocarbonates (**5** and **6**)<sup>7d</sup> with SAA provides evidence for the importance of the electrophilic group in the nucleofuge hierarchy (Scheme 1).

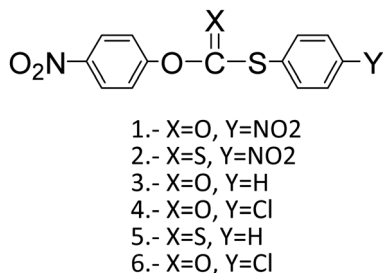
There have been several studies about nucleophilic reactions of diaryl thionocarbonates, *i.e.* in the reactions of 4-cyanophenyl 4-nitrophenyl thionocarbonate (**7**) with phenols<sup>7a</sup> and SAA,<sup>7i</sup> in an aqueous ethanol solution, only 4-nitrophenolate ion is the nucleofuge, suggesting that the p*K*<sub>a</sub> is the reason for this behavior (the difference in the p*K*<sub>a</sub> is 0.9<sup>8</sup>); nevertheless, in the reactions of 4-cyanophenyl 3-nitrophenyl thionocarbonate (**8**) with phenols,<sup>7a</sup> SAA and anilines,<sup>7c</sup> the expulsion of the two *O*-aryl groups was found, (the difference in the p*K*<sub>a</sub> is also 0.9<sup>8</sup>). In the phenolysis reaction of **8**, the ratio 3-nitrophenolate/4-cyanophenolate is 1/3 while the ratio is 2/3 in the aminolysis, providing evidence for the importance of the electrophilic group in the nucleofuge hierarchy.

In this work, we report the differences in the mechanism of SAA aminolysis reactions for two very similar compounds, 4-nitrophenyl 4-cyanophenyl thionocarbonate (**7**) and 4-nitrophenyl 4-cyanophenyl carbonate (**9**) in acetonitrile solution;

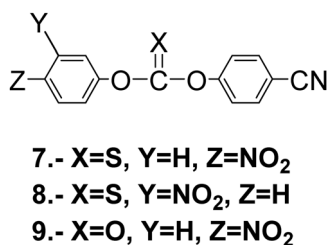
Departamento de Química Física, Facultad de Química y de Farmacia, Pontificia Universidad Católica de Chile, Casilla 306, Santiago, Chile.

E-mail: rmontecino@uc.cl, jgsantos@uc.cl

† Electronic supplementary information (ESI) available. See DOI: 10.1039/d0nj05837h



Scheme 1 Chemical structures of thiol and dithiocarbonates.



Scheme 2 Chemical structures of thionocarbonates and carbonate.

in these cases, the two probable nucleofuges are from the same family (4-nitro and 4-cyanophenolates) and the relative nucleofugality for both phenolate ions and the influence of the solvent in this relative nucleofugalities can be determined. In order to obtain these objectives an experimental (kinetics and analytical) and a theoretical study of the reaction of **7** and **9** with morpholine and piperidine were done (Scheme 2).

## Results and discussion

### Kinetic and mechanism studies

The <sup>1</sup>H-NMR spectrum for the reaction of **9** with excess morpholine in deuterated acetonitrile (see Fig. S1 in ESI<sup>†</sup>) shows the presence of aromatic signals corresponding to morpholine 4-cyanophenyl carbamate (**10**), morpholine 4-nitrophenyl carbamate (**11**), 4-nitrophenolate (**12**), and 4-cyanophenolate (**13**), as detailed in Scheme 3.

In the same way, the <sup>1</sup>H-NMR spectrum for the reaction of **7** with excess morpholine in deuterated acetonitrile (see Fig. S2 in ESI<sup>†</sup>)

shows the presence of aromatic signals corresponding to **12**, **13**, morpholine 4-cyanophenyl thionocarbamate (**14**) and morpholine 4-nitrophenyl thionocarbamate (**15**), which is also shown in Scheme 3. These results demonstrate that the two *O*-aryl groups are nucleofuges for both substrate reactions.

Kinetic spectrophotometric study was carried out, following the spectral changes in the reaction cell (see Fig. S3–S6 in ESI<sup>†</sup>). These reactions obey a first-order equation and pseudo-first-order rate constants (*k*<sub>obs</sub>) were obtained (see Tables S1–S4 in ESI<sup>†</sup>). *k*<sub>obs</sub> vs. [amine] plots are linear according eqn (1), where *k*<sub>0</sub> and *k*<sub>N</sub> are the rate coefficients for the substrates' solvolysis and aminolysis, respectively.

$$k_{\text{obs}} = k_0 + k_{\text{N}}[\text{amine}] \quad (1)$$

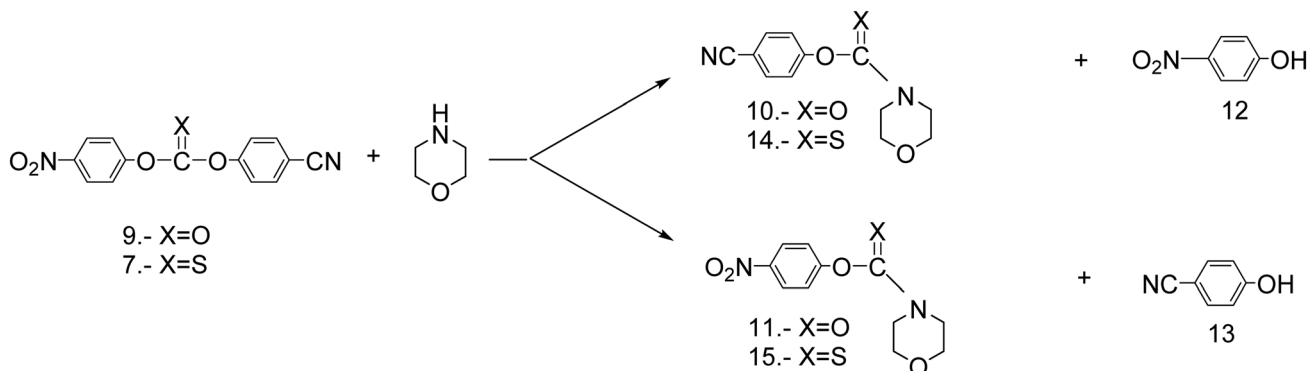
The experimental conditions, amine concentrations and *k*<sub>obs</sub> values obtained for reactions **7** and **9** with SAA in acetonitrile, at 25 °C, are shown in Tables S1 and S2, in the ESI.<sup>†</sup> The values of *k*<sub>0</sub> and *k*<sub>N</sub> were obtained as the intercept and slope, respectively, from the linear plots of *k*<sub>obs</sub> against free amine concentration, eqn (1). The *k*<sub>0</sub> values were much lower than those of the *k*<sub>N</sub> [amine] term in eqn (1). Table 1 shows the second-order rate constants (*k*<sub>N</sub>) for reactions **7** and **9** with SAA and the p*K*<sub>a</sub> of amines (p*K*<sub>a</sub>(ACN)) at 25 °C.

The Brønsted-type plot for the SAA aminolysis of thionocarbonate **7** and carbonate **9** in acetonitrile were obtained (Fig. 1) using the data from Table 1. The *k*<sub>N</sub> values for the reactions with piperazine were corrected because of the two amine groups present in the nucleophile.<sup>10</sup>

As shown in Fig. 1A, the Brønsted-type plot found for the aminolysis of the thionocarbonate **7** is linear, with a slope β value = 0.65. This β value is in agreement with those found for similar concerted reactions (0.4–0.7).<sup>4,7e–h,11</sup>

Nonetheless, the β value by itself is not enough to conclude that a mechanism is concerted. It is also necessary to make sure that the expected p*K*<sub>a</sub> value at the center of the Brønsted curvature (p*K*<sub>a</sub><sup>‡</sup>) for a hypothetical stepwise mechanism is within the p*K*<sub>a</sub> range used.<sup>11</sup>

For the aminolysis reactions of carbonates and their sulfur derivatives reacting through a stepwise mechanism the p*K*<sub>a</sub><sup>‡</sup> value is known to be greater than the p*K*<sub>a</sub> of the leaving group. As the p*K*<sub>a</sub> of 4-nitrophenol and 4-cyanophenol, in acetonitrile,

Scheme 3 Products obtained from the reactions of **7** and **9** with morpholine in acetonitrile solutions.

**Table 1** Acidity constants ( $pK_{a(\text{ACN})}$ ) and second-order rate constants ( $k_N$ ) for reactions **7** and **9** with SAA in acetonitrile (ACN), at 25 °C

AMINES	$pK_{a(\text{ACN})}^{6a,9}$	$k_N/\text{s}^{-1} \text{M}^{-1}$	
		<b>7</b>	<b>9</b>
Morpholine	16.6	$2.5 \pm 0.1$	$1.9 \pm 0.2$
Formylpiperazine	17.0	$11.8 \pm 0.3$	$2.6 \pm 0.1$
1-(2-Hydroxyethyl)piperazine	17.6	$11.9 \pm 0.2$	$4.2 \pm 0.2$
Piperazine	18.5	$82.7 \pm 6$	$25.1 \pm 1$
Piperidine	18.8	$77.3 \pm 2$	$113.4 \pm 4$

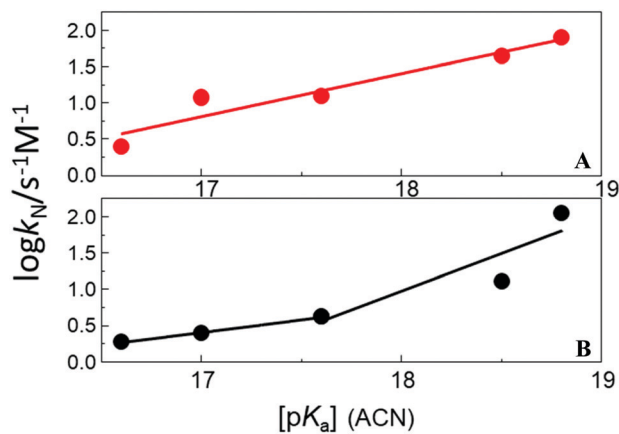
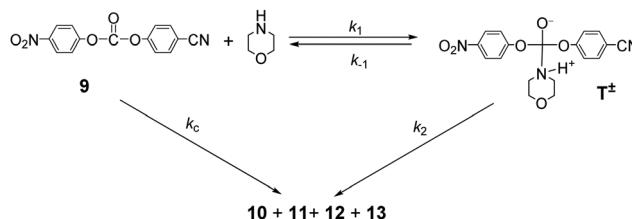


**Fig. 1** Brønsted-type plot for the reactions of SAA with **7** (●; A) and **9** (●; B), in acetonitrile (ACN).

are 20.7 and 22.7, respectively,<sup>12</sup> the  $pK_a^o$  value in acetonitrile would be expected to be greater than 20, which in this case is outside the  $pK_a$  range of the studied amines.

Therefore, if the mechanism were stepwise, the  $\beta = 0.65$  of Fig. 1A would correspond to the expulsion of the leaving group from a tetrahedral intermediate; however, the  $\beta$  value found is too small for this step, confirming the concerted mechanism. Interestingly, the Brønsted plot obtained for aminolysis reaction of **9**, (Fig. 1B), is concave upward. In general, for this kind of nucleophilic substitution reactions, Brønsted plots are linear or biphasic downward, derived from a change in the reaction rate determining step. A concave upward non-linear free energy correlation plot is not frequent and is considered to be a diagnostic of a one reaction with two mechanistic pathways.<sup>13</sup> For instance, Cevasco *et al.* (1985)<sup>13f</sup> showed a concave upward Brønsted plot ( $\log k$  vs.  $pK_{(\text{lg})}$ ) for the hydrolysis reaction of a series of substituted phenyl 4-hydroxybenzoates in aqueous solutions. These results were explained by a  $B_{Ac}2$  mechanism change for poor leaving groups to an  $E_{lc}B$  pathway for good leaving groups. Therefore, the concave upward Brønsted-type plot for reaction of **9** with SAA of Fig. 1B would be associated with the existence of two mechanisms, one concerted and one stepwise, as is shown in Scheme 4, where  $k_c$  is the concerted way and  $k_1$  is the rate constant for the formation zwitterionic intermediate  $T^\ddagger$  by the nucleophilic attack of the amine to the carbonyl moiety of **9** (the stepwise way). Apparently, as the amine basicity increases, the stepwise mechanism is more important.



**Scheme 4** Proposed mechanism for the reaction of carbonate **9** with SAA.

To understand the reactivity patterns and establish how the nucleophile and electrophile structures affect the reaction mechanisms, it is necessary to comprehend how the transition state structures in the rate-determining steps contribute to the dominant mechanistic pathway.<sup>7c,d</sup> Thus, thermodynamic and/or kinetic factors can govern the distribution of products for nucleophilic reactions.<sup>7d,14,15</sup>

Indeed, previous studies have demonstrated that the thermodynamic factor, such as carbon basicity, has a negligible effect on the energy barrier for the aminolysis reactions of dithio-, thionocarbonates and carbonates.<sup>7a,c,d</sup> Accordingly, we have studied the most probable reaction mechanism using the aminolysis reaction of thionocarbonate **7** and carbonate **9** with the nucleophiles morpholine and piperidine as reaction models. In the case of the concerted pathway, the reaction consists of one step, in which all bond-forming and -breaking processes occur simultaneously. Thus, the transition state for the concerted mechanism ( $cTS$ ) involves the simultaneous creation of a C–N bond, cleavage of the C–O bond, and a proton transfer from the amino to the oxygen atom in the nucleofuge. Fig. 2 shows the structures involved in the concerted pathway of the aminolysis of esters.<sup>16</sup> Regarding the reaction model of morpholine with the thionocarbonate, the distance between the thiocarbonyl carbon and the 4-cyanophenol oxygen (nucleofuge) in the transition state structure ( $cTS-7$ ) is much longer, 2.26 Å, than that in compound **7**, 1.35 Å; in the same way, the nitrogen–carbon bond in the  $cTS-7$  has a distance of 1.50 Å, which is greater than the 1.32 Å observed in the thiocarbamate product. Similarly, for the reaction of morpholine with carbonate **9**, the distance between the carbonyl carbon and the 4-cyanophenol oxygen (nucleofuge) in the concerted transition state structure ( $cTS-9$ ) is longer, 2.15 Å, than in compound **9**, 1.35 Å, and the nitrogen–carbon bond in the  $cTS-9$  has a distance of 1.50 Å, which is greater than the 1.35 Å observed in the corresponding thiocarbamate product. The bond lengths of all structures are tabulated in Tables S7–S10 in the ESI.†

On the other hand, the stepwise pathway for the aminolysis of the compounds **7** and **9** corresponds to an addition–elimination

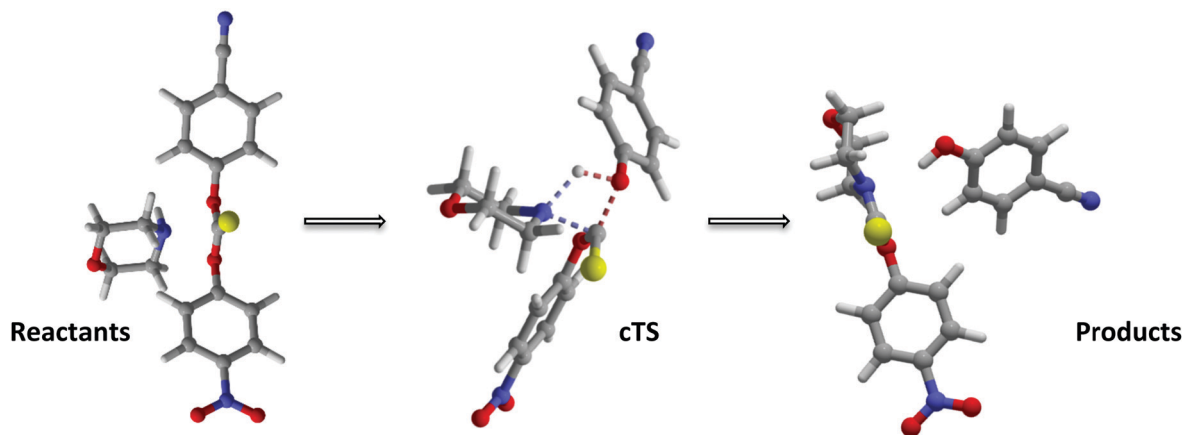


Fig. 2 Optimized structures along the concerted pathway for the aminolysis of compound **7** with morpholine in acetonitrile for the departure of 4-cyanophenol. The dashed lines in the transition state structure **cTS-7** indicates the normal coordinate with one imaginary frequency.

process. Fig. 3 shows the structures along the stepwise pathway for the aminolysis of compound **9** with piperidine. The first step of the reaction is the attack of the piperidine nitrogen on the carbonyl carbon of the carbonate **9**. This addition takes place through a transition state **TS1**. In **TS1**, the C=O double bond becomes slightly longer (1.21 Å) than in the carbonate **9** (1.20 Å). The new C–N bond created has a length of 1.38 Å in **TS1** and 1.45 Å for the intermediate **T±**. The second step corresponds to the conversion of the tetrahedral intermediate into the aminolysis products. The **T±** converts into the carbamates and phenol-derivative products through the transition state **TS2**. This second step involves breaking the C–O single bond and the rehybridization of the carbonyl carbon, accompanied by the nucleofuge expulsion and the proton transfer from the nitrogen atom to the oxygen atom in the nucleofuge. Fig. 3 shows the

stepwise proposal mechanism for the reaction of **9** with piperidine and 4-nitrophenol and the corresponding carbamate as products. The dashed lines correspond to the vibrational motion corresponding to an imaginary frequency in the first (**TS1**) and second transition state (**TS2**), respectively.

Fig. 4 shows the relative Gibbs free energy profiles for stepwise and concerted pathway mechanisms for the aminolysis of compounds **7** and **9** with both amines. Fig. 4 (upper) shows the resulting energy profiles for the reactions of compound **7** with morpholine (left) and with piperidine (right). The black lines are associated to the reactants, the first transition state (**TS1**) and intermediate (**T±**) in the stepwise pathway corresponding to the nucleophilic attack of the morpholine or piperidine to the thiocarbonyl or carbonyl groups in the compounds **7** and **9**, respectively. The red lines represent the transition state associated

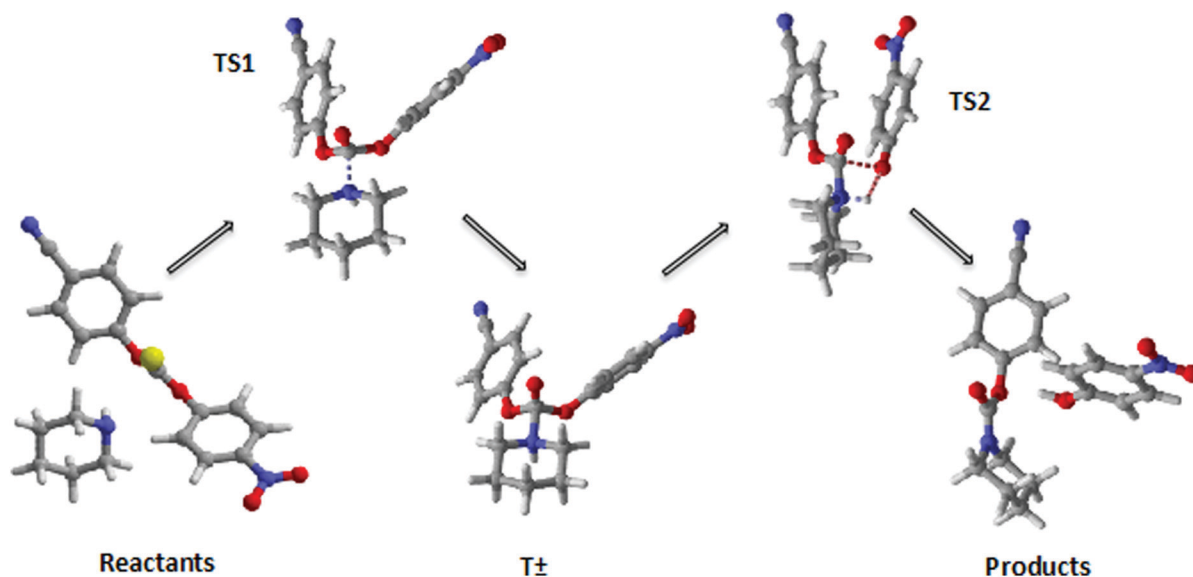


Fig. 3 Structures for the stepwise pathway for the aminolysis of compounds **9** with piperidine in acetonitrile. **TS1** is the transition state between reactants and the zwitterion tetrahedral intermediate **T±**. **TS2** is the transition state between **T±** and 4-nitrophenol and the corresponding carbamate as products. The dashed lines in the transition state structures indicate the normal coordinate with one imaginary frequency.

to the departure of 4-nitrophenol group for concerted (CTS) and stepwise (TS2), while blue lines are used for TS2 associated to the departure of 4-cyanophenol group. For the reactions of **7** and **9** with morpholine (Fig. 4 left), three of the four transition states obtained from the concerted mechanism present lower energy than those observed for the corresponding TS2. These results indicate that both compounds **7** and **9** react with morpholine, preferentially following a concerted mechanism. Interestingly, the comparison of the transition state energies for reactions **7**, and **9** with piperidine show a different behavior (Fig. 4 right). For the reaction of **7** with piperidine, CTS associated to the departure of 4-nitrophenol presents lower energy than TS2, as was observed for the reaction models with morpholine. Nevertheless, in the reaction of **9** with piperidine (Fig. 4, (lower-right)), TS2 for the departure of 4-nitrophenol presents a lower energy level than that observed for CTS, favoring the stepwise mechanism, and confirming the change of mechanism for this reaction. These results agree with

the experimental result in terms of the change of mechanism for the reaction of **9** from a concerted pathway with morpholine to a stepwise pathway with piperidine. Furthermore, in all the systems studied, the relative energies for the departure of the nucleofuge from the corresponding TS were higher for the expulsion of 4-cyanophenol (see Tables S11 and S12 in ESI†). These results, also, predict a higher nucleofugality for 4-nitrophenol compared with 4-cyanophenol for these systems.

The analysis of the bond distances for the different structures for the reactions of compounds **7** and **9** with piperidine or morpholine, including transition states, shows no significant changes that satisfactorily explain the observed change of mechanisms (see Tables S7–S10 in ESI†). Therefore, we studied the molecular charge distribution using the molecular electrostatic potential (MEP) for the reaction models. The colors from red to blue in MEP surface are related to high and low electron density regions, respectively. Fig. 5A and B, show the MEP surface

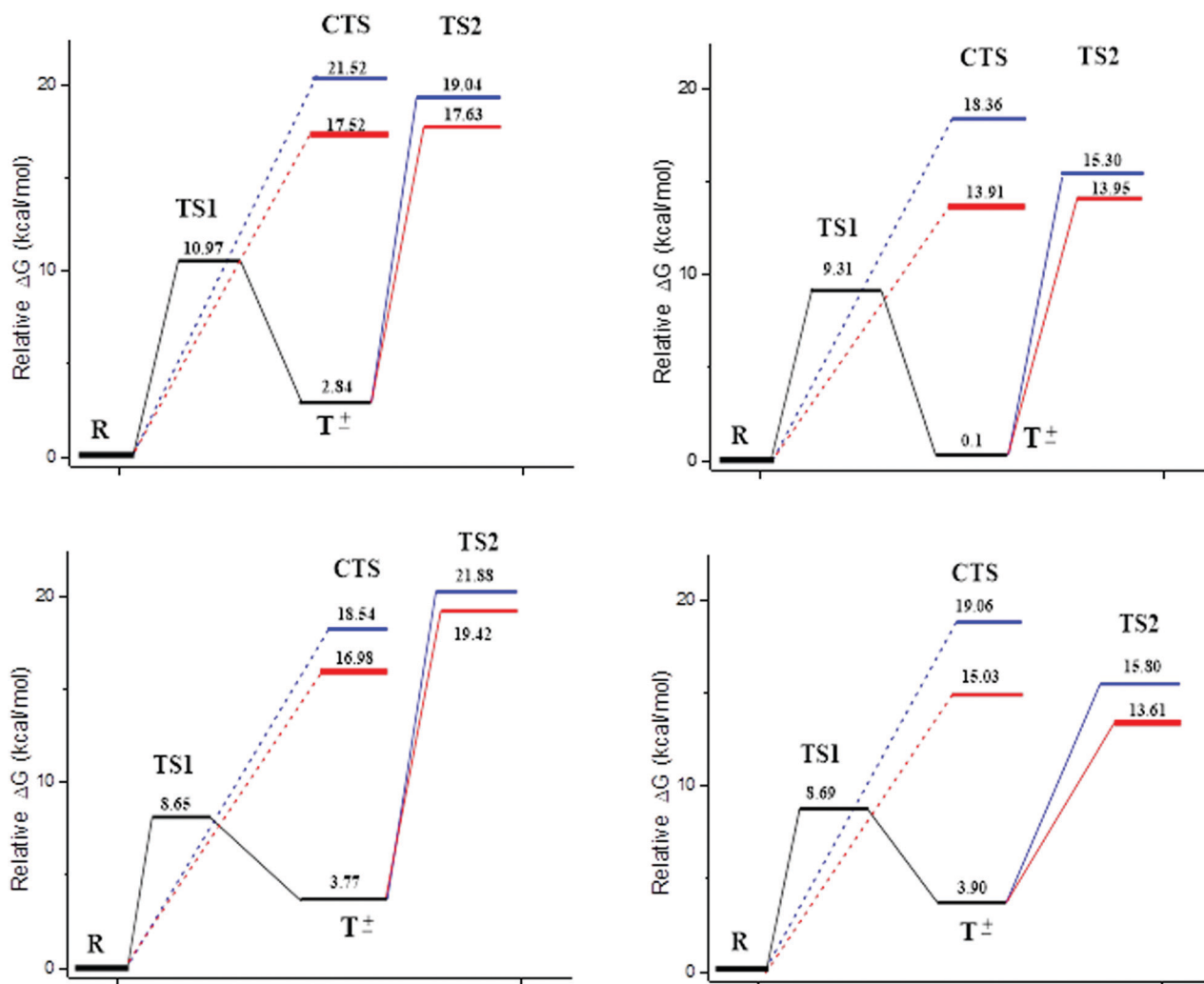


Fig. 4 Relative Gibbs free energy profiles for aminolysis reactions, in acetonitrile, for the thionocarbonate **7** (upper) and carbonate **9** (lower). Left: Energy profiles for the reaction with morpholine. Right: Energy profiles for the reaction with piperidine. Black lines are associated to the reactants (R), first transition state (TS1) and intermediate ( $T^\pm$ ) in the stepwise pathway. Red lines represent the transition state associated with the departure of 4-nitrophenol group in CTS and TS2. Blue lines are related to the departure of 4-cyanophenol group in CTS and TS2. For simplicity products energies are not shown in the profiles.

obtained for the compounds thioncarbonate **7** and carbonate **9**, respectively. From these figures, it is possible to observe an intense red color in the central region for carbonate **9**, where the C=O group is located. This result indicates that the C=O group presents a high electronic polarization, while the C=S (Fig. 5A) shows a weak polarization on these atoms. On the other hand, the MEP maps of the transition states for thioncarbonate with morpholine and piperidine (Fig. 5C and E, respectively) show a lower polarization of the C-S reactive center in comparison with the reactive center of the carbonate **7** (Fig. 5D and F, respectively). Considering that compound **7** reacts with the nucleophiles, preferentially, through a concerted mechanism,

we can infer that structures with a low polarization in the TS would favor the concerted pathway. Likewise, the nature of the amine does not modify the low polarization of the C-S reactive center in the TS, showing that, for this reaction, there is no strong dependence on the properties of the nucleophile, but rather it is the electrophile (C=S) that, with its low polarity, would govern the nucleofuge departure.<sup>17,18</sup> On the other hand, the MEP maps for the TSs of compound **9** with morpholine and piperidine (Fig. 5D and F, respectively) exhibit an interesting difference. For the reaction of compound **9** with morpholine, the reactive center has a less intense red zone than that observed for the reaction with piperidine. Hence, the carbonyl

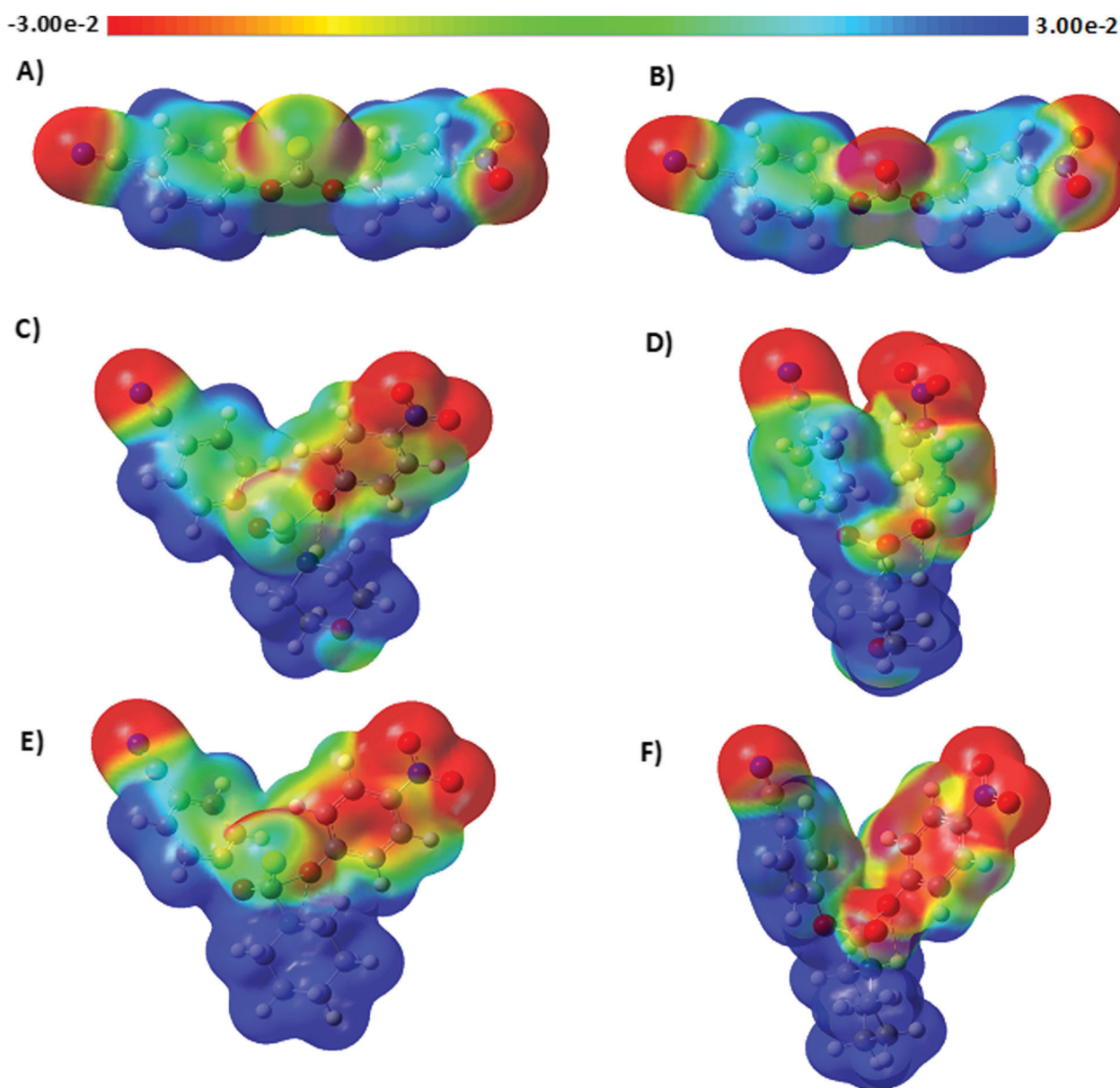


Fig. 5 MEP surfaces mapped onto the isodensity surface for the molecule (A) thioncarbonate **7**; (B) carbonate **9**; (C) TS2: thioncarbonate **7**-morpholine; (D) TS2: carbonate **9**-morpholine; (E) TS2: thioncarbonate **7**-piperidine; (F) TS2: carbonate **9**-piperidine. All MEP surfaces were calculated at the M06-2X/6-31G++(d,p) theory level in acetonitrile (CPCM).

region of **9** with morpholine shows a reduced polarization than that observed with piperidine. In addition, Fig. 5F shows the MEP map with the highest electronic density on the 4-nitrophenolate fragment (nucleofuge). Therefore, the concerted reaction mechanism would be associated with less polarized transition states,<sup>19</sup> while the stepwise mechanism would be related to more polarized transition states. In the same way, the nature of the amine modifies the polarization of the CO reactive center in TS2 (Fig. 5D and F), and it cannot be ruled out for this reaction that both the electrophile polarization and the nucleophilic nature of the amine participates in the nucleofuge departure. Therefore, the stabilization of the reactive group (C=O or C=S and their intermediates) becomes an important parameter for establishing a preferential reaction mechanism.<sup>18,20</sup>

### Solvent effect studies

It is interesting to note that the analysis of the products of the reaction of **7** with morpholine, in aqueous ethanol,<sup>7i</sup> demonstrates that only 4-nitrophenolate is the nucleofuge. The different behaviors of the reaction in aqueous ethanol and in acetonitrile could be attributed to a change in the reaction mechanism, as the first mechanism is stepwise,<sup>7i</sup> while in the latter (this study), the mechanism is concerted. The change of mechanism induced by the change of solvent from polar to less polar can be explained by the great destabilization of the zwitterionic tetrahedral intermediate. In addition, to have a global picture of the solvation effect on the mechanism, the linear free energy relationship (LFER) can provide a good tool to describe solute–solvent interactions.<sup>21</sup> Thus, a solvent-dependent physicochemical property, such as a rate constant, can be correlated with solvation properties of the solvent, such as acidity (HBD solvents), basicity (nonpolar non-HBD solvents) and the polarizability (dipolar non HBD solvents) by using a multiparametric equation. In order to understand the solvent effect in the title reaction in greater depth, we kinetically studied the reaction of **7** and **9** with piperidine in several solvents, with different solvation properties (i) nonpolar solvents (toluene, dioxane), (ii) polar aprotic solvents (acetonitrile, acetone, DMSO, ethyl acetate) and (iii) polar protic solvents (methanol, ethanol, 2-propanol, 2-methyl propanol). The experimental conditions and the pseudo-first-order rate constants are summarized in Tables S3 and S4, in ESI.† Table 2 summarizes the nucleophilic rate constants  $k_N$  for the reaction of **7** and **9** with piperidine in different solvents, showing an important solvent effect. For example, for these reactions, the  $k$  value increase of about 130 and 200 times for **7** and **9**, respectively, by going from toluene to DMSO as solvent.

In a first attempt to understand the solvent effect, we only used the Reichard  $E_T(30)$ <sup>14</sup> parameter of Table 2. Fig. S3, in ESI,† shows the dependence of  $\log k_N$  against  $E_T(30)$  for reactions **7** and **9** with piperidine in different solvents; it can be observed that the  $\log k_N$  values initially increase with  $E_T(30)$  solvents but for alcohols (polar protic solvents) the reaction rate decreases. Further correlations revealed which parameters have the most important impact.

Thus, in order to have a better understanding of solvent effects and to estimate the separate contributions to the

**Table 2** Nucleophilic rate constants  $k_N$  for the reaction of **7** and **9** with piperidine in different solvents, Reichardt solvent polarity parameter ( $E_T(30)$ )<sup>14</sup> and Catalan's solvent properties (SPP, SB, and SA)<sup>22</sup>

Solvent	$k_N/s^{-1} M^{-1}$		Solvent parameters			
	<b>7</b>	<b>9</b>	$E_T(30)^b$	SPP <sup>c</sup>	SB <sup>c</sup>	SA <sup>c</sup>
Toluene	3.9 ± 0.1	18.9 ± 0.5	33.9	0.655	0.128	0
Dioxane	5.9 ± 0.1	28 ± 1	36.0	0.701	0.444	0
Ethyl acetate	23.2 ± 0.6	52 ± 2	38.9	0.795	0.542	0
2-Methyl propanol	6.6 ± 0.2	—	48.6	0.832	0.828	0.311
Isopropanol	9.2 ± 0.2	67 ± 3	48.4	0.848	0.83	0.283
Ethanol	8.9 ± 0.4	52 ± 3	51.9	0.853	0.658	0.400
Methanol	4.6 ± 0.2	65 ± 2	55.4	0.857	0.545	0.605
Acetone	70 ± 2	190 ± 10	42.2	0.881	0.475	0
Acetonitrile	79 ± 2 <sup>a</sup>	114 ± 4 <sup>a</sup>	45.6	0.895	0.286	0.044
DMSO	500 ± 20	3800 ± 300	45.1	1.00	0.647	0.072

<sup>a</sup> Value of Table 1. <sup>b</sup>  $E_T(30)$  is the Dimroth–Reichardt polarity scale. <sup>c</sup> (SA, SB and SPP are Catalan's solvent properties such as the acidity, basicity, and polarizability, respectively).

nucleophilic rate constants for reactions **7** and **9** with piperidine (Table 2), a multiparametric analysis<sup>23</sup> was performed using eqn (2) with the Catalan's parameters (Table 2) (SA, SB and SPP are the acidity, basicity and polarizability, respectively).

$$\log k_N = A_0 + b \times SPP + c \times SA + d \times SB \quad (2)$$

The multiparametric approaches for the solvent effects on the piperidinolysis reaction of **7** lead to the equations shown in Table S5 in ESI.†

Any parameter alone correlates with the experimental results. The best correlation with two parameters was that involving the dipolarity/polarizability SPP and acidity SA parameters according to eqn (3) (eqn (S6), in Table S5 in ESI.†).

$$\log k_N = -(3.7 \pm 0.4) + (6.4 \pm 0.5) \times SPP - (2.0 \pm 0.2) \times SA \quad (3)$$

The incorporation of the solvent basicity (SB) leads to eqn (S7) in Table S5 in ESI,† which increases the  $R$  value; however, there is a decrease in statistical  $F$  factor, and also, the standard error in the calculated SB coefficient is too large. Therefore, we believe that the solvent basicity is not an important factor in the studied reactions. Fig. 6 shows a double logarithmic plot of the experimental nucleophilic rate constant ( $k_{N(\text{exp})}$ ) values against those calculated by eqn (3) ( $k_{N(\text{calc})}$ ). The plot shows, within the experimental errors, a slope = 1 and intercept at the origin, as expected for a good correlation.

The most important contribution to enhancing the rate constant of this reaction is the solvent dipolarity/polarizability (SPP), while increasing solvent acidity (SA) decreases the rate constant. The positive coefficient of SPP in eqn (3) is in accordance with a greater TS stabilization than reactants, leading to less activation energy and consequently an increase in the rate constant.

On the other hand, the negative value of the solvent acidity (SA) coefficient in eqn (3) is in accordance with the ability to donate hydrogen-bonds that would act on the nucleophile/electrophile pair, solvating the nucleophile by hydrogen-bond;<sup>8</sup>

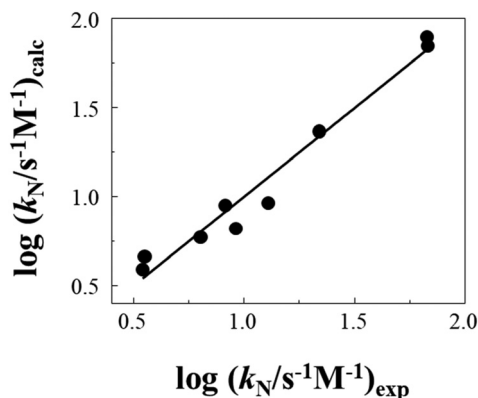


Fig. 6 Double logarithmic plot of  $k_N(\text{exp})$  vs.  $k_N(\text{calc by eqn (3)})$  for the piperidinolysis of **7**.

this effect would increase the activation energy of the reaction, and therefore, decrease the rate constant.

The solvent effect found is according to that observed for the concerted reaction of *O*-ethyl *S*-(2,4-dinitrophenyl) dithiocarbonate with morpholine<sup>24</sup> in which the increase in solvent polarity (SPP) has a positive effect on the second order rate constant, while that of the acidity (SA) solvent parameter has a negative effect on it.

The same statistical study was carried out for the reaction of **9** with piperidine in the different solvents studied (see Table S6 in ESI†).

From the multiparametric statistical study of the reaction of the piperidinolysis for carbonate **9**, the best correlation with two parameters ( $R = 0.88$ ) is that of eqn (4) (eqn (S13) Table S6 in ESI†).

$$\log k_N = -1.4 + 4.1 \times \text{SPP} - 0.6 \times \text{SA} \quad (4)$$

Nevertheless, we must disregard eqn (4) as a solution, because the double logarithmic graph of  $k_N(\text{exp})$  vs.  $k_N(\text{calc by eqn (S13)})$  (Table S6 in ESI†), not shown, presents a slope = 0.538 and an intersection = 0.88, far from the slope = 1 and null intercept required.

Clearly this solvent behavior is not the same as shown by the piperidinolysis of thionocarbonate **7**; probably the piperidinolysis reaction of carbonate **9** proceeds by two mechanistic pathways, depending on the solvents. For this reaction, as shown above, the theoretical calculation indicates that the barrier for TS2 is lower than TS for concerted mechanism.

The change in the mechanism found for the piperidinolysis reaction of carbonate **9** by increasing the polarity of the solvent is in line with that found for thiocarbonate **7**, which changes

from a concerted mechanism in non-aqueous solvents (this study) to one stepwise in 44 wt% ethanol-water.<sup>7i</sup>

### Nucleofugality

Taking into account the fact that the aminolysis reaction of **7** undergoes a change of mechanism from concerted to stepwise when changing the solvent from acetonitrile to 44% p/p aqueous ethanol and that in the latter only 4-nitrophenol behaves as a nucleofuge, the influence of the solvent on the ratio of nucleofuges in the aminolysis reaction of **7** and **9** was assessed. For this purpose, the series of <sup>1</sup>H-NMR spectra were measured for the reactions of **7** and **9** with morpholine and piperidine. These are shown in the Fig. S8–S17 in ESI.† In addition, Table 3 shows the proportion of nucleofuges, ( $P$ ) determined from the ratio of the integration of aromatic proton signals neighboring the nitro group into nitrophenol and nitrophenyl thiocarbamate, respectively.

Firstly, in the reactions of **7** with morpholine, in all the solvents studied, 4-nitrophenolate ion always behaves as a better nucleofuge than 4-cyanophenolate ion ( $P > 1$ ). It is important to note that the calculation, based on the energy barriers (see Fig. 4), allows us to predict the experimental result for the preferential product formation of 4-nitrophenol over 4-cyanophenol in acetonitrile. The preferential product formation can be explained by the capacity of the nitro- as electron-tractor group that induces a more efficient electronic delocalization in the 4-nitrophenolates than the nitrile-group in 4-cyanophenolates, in line with the sigma Hammett values. Therefore, the charge stabilization in the leaving groups, in acetonitrile, could be the main factor that governs the product distribution.

It is also important to state that, within the error in the experimental measurement, the solvent does not affect the products' relation ( $P$  value was kept between 2.1 and 2.5). This result suggests that the relative nucleofugalities are independent of the solvent. There is also a similar quotient ( $P = 2.7$ ) for the piperidinolysis reaction of **7** in acetonitrile. This result suggests that the nucleofuge hierarchy does not change in the amine series.

On the other hand, in the reaction of **9** with morpholine in acetonitrile, the nucleofugality ratio value ( $P = 1.7$ ) is not different than that for the substrate **7** ( $P = 2.4$  in Table 3), probably because the reactions of both substrates with morpholine goes by a concerted mechanism. Nevertheless, in the reaction of **9** with piperidine in acetonitrile ( $P = 13.3$ ), (see Fig. S17, ESI†), this large increase in  $P$  can be seen in the nucleofuge ability of 4-nitrophenol, relative to 4-cyanophenol, probably due to the change of mechanism from concerted to stepwise.

Table 3 Relative nucleofugality 4-nitrophenol/4-cyanophenol ( $P$ ) in the reaction of **7** with morpholine in different deuterated and nondeuterated solvents

Solvent	THF-d <sub>4</sub>	DMSO-d <sub>6</sub>	Acetone-d <sub>6</sub>	CD <sub>3</sub> CN	CD <sub>3</sub> OD	CDCl <sub>3</sub>	CH <sub>3</sub> OH	Acetone	CH <sub>3</sub> CN
$P$	2.1	2.5	2.5	2.4	2.1	2.1	2.4	2.4	2.3

## Conclusions

The reaction of thionocarbonate **7** with SAA in acetonitrile solution presents a linear Brønsted plot with  $\beta = 0.59$ , in line with a concerted mechanism. This was corroborated by the theoretical study in implicit acetonitrile model as solvent. Nevertheless, the concave upward Brønsted plot for the reaction of **9** with SAA in acetonitrile solution is consistent with two mechanistic reaction paths, one concerted and other stepwise, revealing a change of the reaction mechanism. The theoretical study predicts a concerted pathway for the reaction of compound **9** with morpholine and, alternatively, the stepwise pathway would be the preferential mechanism for the reaction of **9** with piperidine.

The solvent behavior found for the piperidinolysis of **7** is as expected for a concerted mechanism; the increase in the solvent polarity (SPP) boosts the second order rate constant and the increase in acidity solvent (SA) decreases it. The theoretical results predict concerted mechanisms for the aminolysis of both thionocarbonate **7** and carbonate **9** with morpholine in the acetonitrile as solvent.

In the reactions of **7** with morpholine in the different solvents, both aryloxy groups are nucleofuges and the 4-nitrophenolate ion nucleofugality is greater than that of 4-cyanophenolate ion, the products' relation ( $P = 2.1$ – $2.5$ ). This result suggests that the relative nucleofugalities are independent of the solvent. There is also a similar quotient ( $P = 2.7$ ) for the piperidinolysis reaction of **7** in acetonitrile. This result suggests that the nucleofuge hierarchy does not change in the amine series. All these reactions are concerted. These results are also predicted by the theoretical study.

The relative nucleofugality 4-nitrophenol/4-cyanophenol in the reaction of **9** with morpholine and piperidine in acetonitrile changes from 2.7 to 13.2, due to the change of mechanism from concerted to stepwise. In summary, from the results of this study we can conclude that the use of nucleofugality scales is conditioned by the reaction mechanism, rather than by the solvent used.

## Experimental

### Materials

Secondary alicyclic amines (SAA) were purified by recrystallization or distillation. The thionocarbonate **7** was prepared by a literature method<sup>7i,25</sup> and identified by <sup>1</sup>H NMR and IR analyses.<sup>7i</sup>

The carbonate **9** was prepared by a literature method<sup>25</sup> and identified by <sup>1</sup>H NMR and <sup>13</sup>C NMR analyses.<sup>26</sup>

### Kinetic measurements

The kinetics of the reactions were analyzed through a diode array spectrophotometer; some representative examples are presented in Fig. S3–S6 (ESI<sup>†</sup>), following the absorbance increase at a wavelength where the change was greater (see experimental curves in Fig. S3–S6, ESI<sup>†</sup>). All reactions were studied at  $25.0 \pm 0.1$  °C, under at least a 10-fold amine excess over the substrate, with the initial concentration of the latter being  $2.7 \times 10^{-5}$  M and  $3.0 \times 10^{-5}$  M for the reactions of **7** and **9**, respectively.

In all cases, under amine excess, pseudo-first-order rate coefficients ( $k_{\text{obs}}$ ) were obtained adjusting the experimental absorbance time curves to a first order kinetic equation (see the calculated curves in Fig. S3–S6, ESI<sup>†</sup>). The nucleophilic rate constants ( $k_{\text{N}}$ ) were determined from the slopes of linear plots of  $k_{\text{obs}}$  vs. amine concentration.

### Product studies

**High performance liquid chromatography (HPLC).** These were carried out by a diode array detector, provided with LiChroCART<sup>®</sup>250-4 HPLC-RP-18e (5  $\mu\text{m}$ ) HPLC Cartridge LiChrosphere<sup>®</sup>100 RP 8, mobile phase 50% v/v CH<sub>3</sub>CN: phosphate buffer (0.01 M/pH = 7.00), flow rate 1.5 mL/min. The products were identified by comparison of their spectra and retention times (r.t.) with those of authentic samples (see Fig. S18 in ESI<sup>†</sup>).

### Nuclear magnetic resonance

In order to determine the products of the studied reactions, <sup>1</sup>H-NMR spectra were obtained on an AM-400 instrument in <sup>1</sup>H-NMR signals in the aromatic region of the reactions of substrates and those for the expected products for the reactions were assigned by comparison with those of authentic samples. The expected products **10**, **11**, **14** and **15** were prepared *in situ* by the reactions of 4-cyanophenyl chloroformate, 4-nitrophenyl chloroformate, 4-cyanophenyl chlorothioformate and 4-nitrophenyl chlorothioformate with morpholine, respectively.

### Theoretical methods

DFT calculations were carried out in order to explain the origins of the mechanism change and nucleofuge hierarchy for the reaction models. In particular, the studies consider the analysis of concerted and stepwise pathways for the reactions of thionocarbonate **7** and carbonate **9** with morpholine and piperidine.

DFT calculations were performed with the GAUSSIAN 09 program package.<sup>27</sup> All reactants, products, intermediates, and transition state structures were optimized at the M06-2X level of theory using the 6-31G++(d,p) basis set. All the optimizations were carried out in acetonitrile by using the polarized continuum model (SCRF = CPCM).<sup>28</sup> The search for each lowest energy of the reactants, zwitterionic tetrahedral intermediate and products were manually changing the initial geometries and by comparing the resulting optimized structures and energies using a theory/basis set at the M06-2X/6-31G++(d,p) level. Similar procedures for locating the lowest energy structures have been reported in previous works.<sup>7c,d</sup>

To verify the nature of stationary points, vibrational frequency computations were carried out at the same level of theory. Transition states were verified by obtaining only one imaginary frequency at the same level of theory. CYLView software was used for the visualization of structures involved in the reaction mechanism.<sup>29</sup>

## Conflicts of interest

There are no conflicts to declare.

## Acknowledgements

This work was supported by FONDECYT grants 1160271, 1170976 and 1171870. Powered@NLHPC: this research was partially supported by the supercomputing infrastructure of the NLHPC (ECM-02).

## References

- (a) N. Streidl, B. Denegri, O. Kronja and H. Mayr, *Acc. Chem. Res.*, 2010, **43**, 1537–1549; (b) B. Denegri, A. R. Ofial, S. Juri, A. Streiter, O. Kronja and H. Mayr, *Chem. – Eur. J.*, 2006, **12**, 1648–1656.
- (a) M. Matic, B. Denegri and O. Kronja, *Eur. J. Org. Chem.*, 2010, 6019–6024; (b) M. Matic, N. Bebek, B. Denegri and O. Kronja, *Croat. Chem. Acta*, 2016, **89**, 355–362; (c) B. Denegri, M. Matic and O. Kronja, *Synthesis*, 2017, 3422–3432; (d) R. J. Mayer, M. Breugst, N. Hampel, A. R. Ofial and H. Mayr, *J. Org. Chem.*, 2019, **84**, 8837–8858.
- E. A. Castro, *Chem. Rev.*, 1999, **99**, 3505–3524, and references therein.
- A. Williams, *Chem. Soc. Rev.*, 1994, 93–100; A. Williams, *Concerted Organic and Bio-Organic Mechanisms*, CRC Press, Boca Raton, FL, 2000; A. Williams, *Free energy relationships in organic and bioorganic chemistry*, RSC, Cambridge, 2003.
- W. P. Jencks, *Catalysis in Chemistry and Enzymology*, McGraw-Hill, New York, 1969; W. P. Jencks and M. Gilchrist, *J. Am. Chem. Soc.*, 1968, **90**, 2622–2637; B. D. Song and W. P. Jencks, *J. Am. Chem. Soc.*, 1989, **111**, 8479–8484; J. P. Fox and W. P. Jencks, *J. Am. Chem. Soc.*, 1974, **96**, 1436–1449; A. C. Satterthwait and W. P. Jencks, *J. Am. Chem. Soc.*, 1974, **96**, 7018–7031; M. J. Gresser and W. P. Jencks, *J. Am. Chem. Soc.*, 1977, **99**, 6963–6970; M. J. Gresser and W. P. Jencks, *J. Am. Chem. Soc.*, 1977, **99**, 6970–6980.
- (a) I.-H. Um, H.-W. Yoon, J.-S. Lee, H.-J. Moon and D.-S. Kwon, *J. Org. Chem.*, 1997, **62**, 5939–5944; (b) I.-H. Um, K.-H. Kim, H.-R. Park, M. Fujio and Y. Tsuno, *J. Org. Chem.*, 2004, **69**, 3937–3942; (c) I.-H. Um, Y.-M. Fujio, M. Park, M. Mishima and Y. Tsuno, *J. Org. Chem.*, 2007, **72**, 4816–4821; (d) I.-H. Um and A.-R. Bae, *J. Org. Chem.*, 2011, **76**, 7510–7515; (e) I.-H. Um, A.-R. Bae and T.-I. Um, *J. Org. Chem.*, 2014, **79**, 1206–1212; (f) I.-H. Um, M.-Y. Kim, A.-R. Bae, J. M. Dust and E. Bunzel, *J. Org. Chem.*, 2015, **80**, 217–222; (g) I.-H. Um, J.-H. Song, A.-R. Bae and J. M. Dust, *Can. J. Chem.*, 2018, **96**, 1011–1020.
- (a) E. A. Castro, A. Cañete, P. R. Campodónico, M. Cepeda, P. Pavez, R. Contreras and J. G. Santos, *Chem. Phys. Lett.*, 2013, **572**, 130–135; (b) E. A. Castro, M. E. Aliaga, M. Gazitúa, P. Pavez and J. G. Santos, *J. Phys. Org. Chem.*, 2014, **27**, 265–268; (c) R. Montecinos, M. E. Aliaga, P. Pavez and J. G. Santos, *New J. Chem.*, 2017, **41**, 9954–9962; (d) R. Montecinos, M. Gazitúa and J. G. Santos, *New J. Chem.*, 2019, **43**, 6372–6379; (e) E. A. Castro, M. Aliaga, P. Campodónico and J. G. Santos, *J. Org. Chem.*, 2002, **67**, 8911–8916; (f) E. A. Castro, M. Gazitúa and J. G. Santos, *J. Org. Chem.*, 2005, **70**, 8088–8092; (g) E. A. Castro, M. Ramos and J. G. Santos, *J. Org. Chem.*, 2009, **74**, 6374–6377; (h) E. A. Castro, M. Cubillos, R. Iglesias and J. G. Santos, *Int. J. Chem. Kinet.*, 2012, **44**, 604–611; (i) E. A. Castro, L. Leandro, N. Quesieh and J. G. Santos, *J. Org. Chem.*, 2001, **66**, 6130–6135; (j) J. G. Santos and M. Gazitúa, *J. Phys. Org. Chem.*, 2019, **32**, e3818; (k) E. A. Castro, M. E. Aliaga, M. Gazitúa and J. G. Santos, *J. Phys. Org. Chem.*, 2012, **25**, 994–997; (l) E. A. Castro, M. Cepeda, P. Pavez and J. G. Santos, *J. Phys. Org. Chem.*, 2009, **22**, 454–459.
- A. Albert and E. P. Serjeant, *The Determination of Ionization Constants* Chapman and Hall, London, 1971, p. 87.
- W. J. Spillane, P. McGrath, D. Brack and A. B. O'Byrne, *J. Org. Chem.*, 2001, **66**, 6313–6316.
- R. P. Bell, *The proton in chemistry*, Cornell University Press, 1973.
- E. Chystiuk and A. Williams, *J. Am. Chem. Soc.*, 1987, **109**, 3040–3046; A. Williams, *Acc. Chem. Res.*, 1989, **22**, 387–392; S. Ba-Saif, A. K. Luthra and A. Williams, *J. Am. Chem. Soc.*, 1989, **111**, 2647–2652.
- I. M. Kolthoff and M. K. Chantooni Jr, *J. Am. Chem. Soc.*, 1969, **91**, 4621–4625; J. Magonsky, Z. Paulak and T. Jasinsky, *J. Chem. Soc., Faraday Trans.*, 1993, **89**, 119–122; F. Eckert, I. Leito, I. Kaljurand, A. Kutt, A. Klamt and M. Diedenhofen, *J. Comput. Chem.*, 2009, **30**, 799–810.
- (a) K. K. Adhikary and H. W. Lee, *Bull. Korean Chem. Soc.*, 2011, **32**, 857–862; (b) N. El Guesmi, G. Berionni and B. H. Asghar, *Monatsh. Chem.*, 2013, **144**, 1537–1545; (c) M. E. U. Hoque and H. W. Lee, *Bull. Korean Chem. Soc.*, 2012, **33**, 325–328; (d) M. E. U. Hoque, N. K. Dey, A. K. Guha, C. K. Kim, B. S. Lee and H. W. Lee, *Bull. Korean Chem. Soc.*, 2007, **28**, 1797; (e) H. R. Barai and H. W. Lee, *Bull. Korean Chem. Soc.*, 2012, **33**, 309–312; (f) G. Cevasco, G. Guanti, A. R. Hopkins, S. Thea and A. Williams, *J. Org. Chem.*, 1985, **50**, 479–484.
- H. Mayr and A. R. Ofial, *Acc. Chem. Res.*, 2016, **49**, 952–965.
- J. Hine and R. D. Weimar, *J. Am. Chem. Soc.*, 1965, **87**, 3387–3396.
- S. Ilieva, B. Galabov, D. G. Musaev, K. Morokuma and H. F. Schaefer III, *J. Org. Chem.*, 2003, **68**, 1496–1502.
- T. A. Hamlin, M. Swart and F. M. Bickelhaupt, *ChemPhysChem*, 2018, **19**, 1315–1330.
- A. R. Katritzky, O. Meth-Cohn and C. H. Rees, *Comprehensive Organic Functional Group Transformations, Synthesis: Carbon with One Heteroatom Attached by a Multiple Bond*, Elsevier, 2003, vol. 3.
- M. Alves, R. Mereau, B. Grignard, C. Detrembleur, C. Jerome and T. Tassaing, *RSC Adv.*, 2017, **7**, 18993–19001.
- M. Y. Kim and I. H. Um, *Bull. Korean Chem. Soc.*, 2016, **37**, 1401–1405.
- C. Reichardt and T. Welton, *Solvents and Solvent Effects in Organic Chemistry*, Wiley VCH Verlag & Co., Weinheim, German, 4th edn, 2011.
- J. Catalán, V. López, P. Pérez, R. Martín-Villamil and J. G. Rodríguez, *Liebigs Ann.*, 1995, 241–252; J. Catalán, C. Díaz, V. López, P. Pérez, J. L. G. De Paz and J. G. Rodríguez, *Liebigs Ann.*, 1996, 1785–1794; J. Catalán and C. Díaz, *Liebigs Ann.*, 1997, 1941–1949.

- 23 I. A. Koppel and V. A. Palm, in *Advances in linear free energy relationships*, ed. N.V. Chapman and J. Shorter, Plenum Press, New York, 1972, p. 222.
- 24 D. Millán, J. G. Santos and E. A. Castro, *J. Phys. Org. Chem.*, 2012, **25**, 989–993.
- 25 H. R. Al-Kazimi, D. S. Tarbel and D. A. Plant, *J. Am. Chem. Soc.*, 1955, **77**, 2479–2482.
- 26 J. G. Santos, M. E. Aliaga, M. F. Márquez and M. Oyarzún, *J. Phys. Org. Chem.*, 2019, **32**, e3845.
- 27 M. J. Frisch, G. W. Trucks, H. B. Schlegel, G. E. Scuseria, M. A. Robb, J. R. Cheeseman, G. Scalmani, V. Barone, B. Mennucci, G. A. Petersson, H. Nakatsuji, M. Caricato, X. Li, H. P. Hratchian, A. F. Izmaylov, J. Bloino, G. Zheng, J. L. Sonnenberg, M. Hada, M. Ehara, K. Toyota, R. Fukuda, J. Hasegawa, M. Ishida, T. Nakajima, Y. Honda, O. Kitao, H. Nakai, T. Vreven, J. A. Montgomery Jr, J. E. Peralta, F. Ogliaro, M. Bearpark, J. J. Heyd, E. Brothers, K. N. Kudin, V. N. Staroverov, R. Kobayashi, J. Normand, K. Raghavachari, A. Rendell, J. C. Burant, S. S. Iyengar, J. Tomasi, M. Cossi, N. Rega, M. J. Millam, M. Klene, J. E. Knox, J. B. Cross, V. Bakken, C. Adamo, J. Jaramillo, R. Gomperts, R. E. Stratmann, O. Yazyev, A. J. Austin, R. Cammi, C. Pomelli, J. W. Ochterski, R. L. Martin, K. Morokuma, V. G. Zakrzewski, G. A. Voth, P. Salvador, J. J. Dannenberg, S. Dapprich, A. D. Daniels, O. Farkas, J. B. Foresman, J. V. Ortiz, J. Cioslowski and D. J. Fox, *Gaussian09, Revision D.01*, Gaussian, Inc., Wallingford, CT, 2013.
- 28 M. Garcia-Ratés and F. J. Neese, *Comput. Chem.*, 2020, **41**, 922–939.
- 29 C. Y. Legault, *CYLVview20*, Université de Sherbrooke, 2020. <http://www.cylvview.org>.